Rapid calculation of the ion energy distribution on a plasma electrode

Paola Diomede,[a] Demetre J. Economou,[b] and Vincent M. Donnelly[c]
Plasma Processing Laboratory, Department of Chemical and Biomolecular Engineering, University of Houston, Houston, Texas 77204-4004, USA

(Received 19 March 2012; accepted 5 May 2012; published online 27 June 2012)

A model was developed to rapidly calculate the ion energy distribution (IED) on an electrode immersed in plasma, for a given voltage waveform applied to the electrode through a blocking capacitor. The model combined an equivalent circuit representation of the system, with an equation for a damped potential to which ions respond, during their transit through the sheath. Predicted IEDs on both conducting and insulating surfaces for a variety of applied voltage waveforms (spike, staircase, square wave, etc.) agreed with published experimental data. For these comparisons with experiments, peak broadening due to the resolution of the ion energy analyzer was also taken into account. Using "tailored" waveforms of the applied voltage, desired IEDs may be obtained in terms of peak energies and fraction of ions under each peak. *© 2012 American Institute of Physics*. [http://dx.doi.org/10.1063/1.4728997]

I. INTRODUCTION

The energy of ions bombarding the substrate during plasma etching is important to both etching rate and selectivity. Selectivity of etching the substrate vs. the underlying layer (or the photoresist mask) may be achieved if the ion energy is set between the threshold energies for etching these materials. The ion energy must be high enough to promote ion-assisted chemistry on the substrate, but not excessively high to compromise selectivity or induce substrate damage.

The ion energy distribution (IED) depends, among other variables, on the sheath voltage and the applied frequency. For a sinusoidal voltage and a collisionless sheath, the relevant parameter is $\frac{\tau_i}{\tau_{rf}} = \frac{3s\omega}{2\pi}\left(\frac{M}{2eV_s}\right)^{1/2}$ the ratio of the ion transit time through the sheath, τ_i, to the period of the applied rf, τ_{rf}.[1–3] Here, s, ω, M, and V_s are time-average sheath thickness, applied voltage angular frequency, ion mass, and time-average sheath voltage, respectively. When $\tau_i/\tau_{rf} \ll 1$, ions respond to the instantaneous sheath voltage, and the IED has a large energy spread. When $\tau_i/\tau_{rf} \gg 1$, ions respond to an average (damped) sheath voltage, and the IED becomes narrow. A nearly monoenergetic IED is often required for high selectivity because the threshold ion energies for etching a variety of materials are not very different from one another. In the case of sinusoidal applied voltage, the width of the distribution may be decreased by increasing the frequency, ω.

Nearly monoenergetic IEDs (with narrow full width at half maximum, FWHM), were reported by Xu *et al.*[4] and Shin *et al.*[5] They applied a dc bias voltage on a "boundary electrode" during part of the afterglow of a pulsed plasma. The electron temperature T_e drops precipitously in the afterglow and, since the width of the IED scales with T_e,[6] the FWHM can be minimized, especially in the late afterglow. Simulation predictions[7] were in good quantitative agreement with measurements.[4]

The IED may also be controlled by applying a judicious voltage waveform (not necessarily sinusoidal) on the substrate electrode. Earlier studies used asymmetric rectangular voltage pulses, whereby charging of dielectric substrates was minimized by shortening the pulse duration.[8–10] Wendt and co-workers[11–14] applied a low frequency impulse waveform or a square waveform on a substrate immersed in a continuous wave plasma to obtain a peaked IED. The waveform had to be given the right slope to account for charging of non-conductive substrates, and still yield a nearly constant sheath potential, and thus a nearly monoenergetic IED, in the limit $\tau_i/\tau_{rf} \ll 1$. A similar approach was used by Kudlacek *et al.*[15] who also studied the influence of substrate charging on the required voltage waveform,[16,17] so that monoenergetic IEDs are obtained. Agarwal and Kushner[18] and Rauf[19] conducted computational investigations of the effect of non-sinusoidal bias voltage waveforms on the IED, etching rate and selectivity. Moreover, the application of tailored rf voltage waveforms was shown to generate a controlled electrical asymmetry in a capacitively coupled PECVD system.[20] A shift in the dc bias voltage (indicating asymmetric distribution of the sheath voltages) was observed when inverting the voltage waveform shape from "peaks" to "troughs." It was found that by increasing or decreasing the ion bombardment energy, the film growth switched between amorphous silicon and nanocrystalline silicon.

Diomede *et al.* conducted a particle-in-cell simulation with Monte Carlo Collisions (PIC-MCC) of the application of tailored dc voltage steps on an electrode, during the afterglow of a capacitively coupled pulsed-plasma, to control the energy of ions incident on the counter-electrode.[21] Staircase voltage waveforms with selected amplitudes and durations resulted in IEDs with distinct narrow peaks, each with controlled energy. Although PIC-MCC is ideal for obtaining the IEDs, it requires long computational time (e.g., hours or even days). In the present work, a model is presented to

[a]padiomede@gmail.com.
[b]economou@uh.edu.
[c]vmdonnelly@uh.edu.

 © 2012 American Institute of Physics

Downloaded 03 Jul 2012 to 129.7.205.168. Redistribution subject to AIP license or copyright; see http://jap.aip.org/about/rights_and_permissions

rapidly (e.g., seconds) compute the IED on a substrate in contact with plasma, under the influence of an applied voltage waveform.

II. MODEL DEVELOPMENT

The system under study is shown in Fig. 1. An electrode (target) is in contact with a plasma with given electron temperature (T_e) and electron density (n_0) in the bulk (away from the electrode surface). A RF bias of the desired waveform (V_{rf}) is applied to the target electrode through a blocking capacitor (C_b). It was assumed that the applied bias is small enough not to perturb the given bulk electron density and temperature. It was further assumed that the plasma is electropositive with one kind of positive ion, suffering no collisions in the sheath. In addition to the target electrode (area A_T), the plasma reactor system also includes a "counter-electrode" (area A_G), which is often grounded. Although the target bias voltage was assumed small enough not to alter the bulk electron density or electron temperature, the plasma potential may be affected, depending on the area ratio, A_G/A_T. For large values of this ratio, the plasma potential will be near ground. In general, floating surfaces may also be in contact with the plasma. Thus, the ratio A_G/A_T may have to be regarded as an "effective" area ratio, so that the electrical characteristics of the actual system are reproduced by the model. The goal is to determine the ion energy distribution on the target electrode given n_0, T_e, V_{rf}, C_b, and the electrode area ratio A_T/A_G. This is accomplished by following four steps: (a) an equivalent circuit model is used to calculate the sheath potential over the target electrode; (b) the latter is used in an equation for the "damped" sheath potential to which ions respond; (c) knowing the damped sheath potential, the IED is calculated; and (d) instrumental broadening is applied to arrive at the IED on the target electrode. Each of these steps is described below. It should be noted that, in the case of dc coupling of the voltage source to the electrode (no blocking capacitor), the area ratio has no influence on the results. It is also noted that the problem described above is the "forward" problem of finding the IED. The "inverse" problem, i.e., that of finding the voltage waveform that must be applied to achieve a desired (preselected) IED on the target electrode is discussed in Ref. 22.

A. Equivalent circuit model

An equivalent circuit model (Fig. 2) was used as described by Metze *et al.*[23,24] The sheath was modeled as a capacitor in parallel with a current source and a diode. The current source represents the ion current and the diode represents the electron current. Subscripts T and G denote the target electrode and the grounded electrode, respectively. V_p is the plasma potential. The sheath capacitance was described as a non-linear function of the sheath potential (Eq. (4) below).

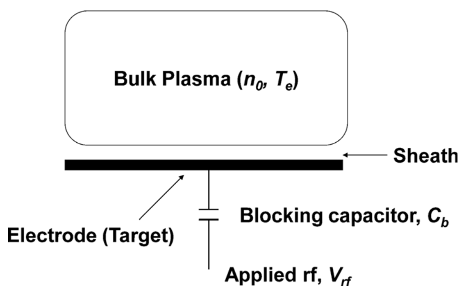

FIG. 1. Schematic of the system under study.

Applying Kirchhoff's law to this circuit yields

$$
\begin{aligned}
C_b \frac{d}{dt}(V_{rf} - V_T) + C_T \frac{d}{dt}(V_p - V_T) + I_T = 0, \\
C_T \frac{d}{dt}(V_p - V_T) + C_G \frac{d}{dt} V_p + I_T + I_G = 0,
\end{aligned}
\tag{1}
$$

where V, C, and I are voltage, capacitance, and total particle current to an electrode, respectively. The particle current is the sum of the ion and electron currents. The former is given by the Bohm flux, while the latter is found from the thermal electron flux at the wall. For the target electrode,

$$
\begin{aligned}
I_T &= A_T(J_i + J_e) = A_T e n_0 \\
&\times \left[0.605 u_B - \frac{1}{4} u_e \exp\left(e \frac{V_T - V_p}{kT_e}\right)\right],
\end{aligned}
\tag{2}
$$

where A_T is the area of the target electrode, u_B is the Bohm speed ($u_B = \sqrt{kT_e/M}$), M is the ion mass, u_e is the electron thermal speed ($u_e = \sqrt{\frac{8kT_e}{\pi m}}$), and m is the electron mass. The factor 0.605 accounts for the drop off in plasma density from the bulk plasma to the plasma-sheath interface. When applied to the grounded electrode, the particle current reads

$$
I_G = A_G(J_i + J_e) = A_G e n_0 \left[0.605 u_B - \frac{1}{4} u_e \exp\left(-e \frac{V_p}{kT_e}\right)\right].
\tag{3}
$$

The sheath capacitance is given by

$$
C_s = -\varepsilon_0 A \frac{\partial E}{\partial V_s},
\tag{4}
$$

where the electric field at the wall is[25]

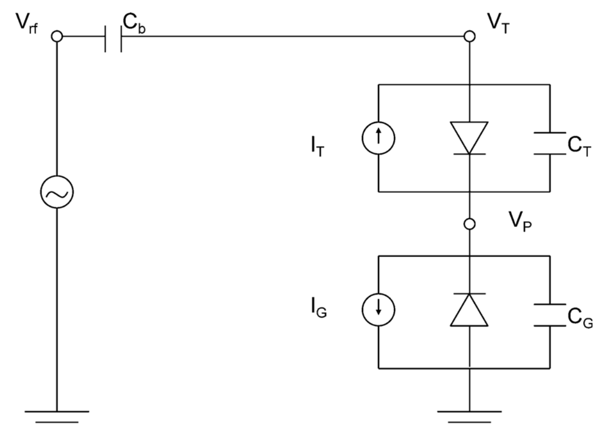

FIG. 2. Equivalent circuit of the system under study. C is capacitance and I is current. Subscripts T and G refer to the target and grounded electrode, respectively.

Downloaded 03 Jul 2012 to 129.7.205.168. Redistribution subject to AIP license or copyright; see http://jap.aip.org/about/rights_and_permissions

$$
\begin{aligned}
&E = -\sqrt{\frac{2n_s kT_e}{\varepsilon_0}}\left(\frac{(\bar{u}-1)}{\bar{\chi}}(1+\chi-e^{\chi})\right)^{1/2}, \\
&\chi = e(V_s - V_1)/kT_e, && \text{for } -\infty < V_s(t) < V_1 \\
&\bar{\chi} = e(V_d - V_1)/kT_e, \\
&\bar{u} = (1-2\bar{\chi})^{1/2}, \\
&E = 0, && \text{for } V_1 \le V_s(t) \le V_p.
\end{aligned} \tag{5}
$$

Here, V_s (≤ 0) is the sheath voltage, ε_0 is the permittivity of free space, n_s is the electron (ion) density at the sheath edge ($n_s = 0.605\, n_0$), and V_1 is the potential at the sheath edge relative to the plasma potential. V_{rf} was used as input to Eq. (1) to find the target V_T and plasma V_p potentials, thus the (actual) sheath voltage ($V_T - V_p$). The latter was subsequently used to find the "damped" sheath voltage to which ions respond.

In the presence of an insulating film on the target electrode, the film capacitance will be in series with the corresponding sheath capacitance. Insulating reactor walls (backed by a grounded surface) could be represented with another "leg" in parallel to that of the grounded electrode of Fig. 2 (see Ref. 26, p. 170). Alternatively, one may employ an "effective" area ratio A_G/A_T and treat it as an adjustable parameter. It should be mentioned that, at very low frequencies (well below the ion plasma frequency), the ion flux entering the sheath is not constant but it is time modulated.[27] This complication was not accounted for in the present model.

B. The "damped" sheath potential

Ions, in general, do not respond to the instantaneous sheath potential, but to a "damped" potential $V_d(x, t)$ found from the following equation:[1,2,25]

$$\frac{dV_d(x,t)}{dt} = -\frac{V_d(x,t) - V(x,t)}{\tau_i}, \tag{6}$$

where $V(x,t)$ is the (actual) sheath potential as a function of position and time and τ_i is the ion transit time through the sheath. This is often approximated by the inverse of the ion plasma frequency at the sheath edge, $1/\omega_{pi}$.[2,3,25] This differential equation applies at any position in the sheath, including the electrode. When applied to the target electrode this equation becomes (omitting x and t for simplicity),

$$\frac{dV_d}{dt} = -\frac{V_d - (V_T - V_p)}{\tau_i}. \tag{7}$$

Since ions respond to the damped potential, the energy distribution of ions striking the target is a direct reflection of that potential. In Eq. (7), $V_T - V_p$ is the actual sheath voltage at the target electrode, i.e., the difference between the target potential V_T and the plasma potential, V_p.

C. Calculation of the IED

The damped sheath voltage waveform $V_d(t)$ found by Eq. (7) above was then used to find the ion energy distribution,[1,22]

$$P(E) = \frac{1}{2\pi} \sum_{\substack{\#\text{ of points in } 0<\omega t<2\pi \\ \text{such that} \\ |eV_d(\omega t)|=E}} \frac{1}{\left|\frac{dV_d}{d(\omega t)}\right|}. \tag{8}$$

D. Instrumental broadening of the IED

Broadening due to the finite energy resolution of the instrument used to measure the IED (for example, electrostatic energy analyzer) was described by an instrument function $h_{E'}(E)$,[28] for which a Gaussian distribution was assumed,

$$h_{E'}(E) = \frac{1}{\delta\sqrt{2\pi}} \exp\left(-\frac{(E-E')^2}{2\delta^2}\right), \tag{9}$$

where E' is the peak ion energy, and δ is the standard deviation of the Gaussian, which is related to the energy resolution ΔE of the instrument by

$$\delta = \frac{\Delta E}{2\sqrt{2\ln 2}}. \tag{10}$$

The IED was found as the convolution of $P(E)$ obtained from Eq. (8) and the instrument function, i.e.,

$$f(E) = P * h_{E'} = \int_0^\infty P(E') \cdot h_{E'}(E) \cdot dE'. \tag{11}$$

Calculation of the IED and the damped and sheath potential waveforms, for given applied voltage waveform, typically took about 5 seconds on a PC employing an Intel Xeon CPU at 2.40 GHz.

III. RESULTS AND DISCUSSION

A. Spikes and staircases

Wendt and co-workers[11] reported IEDs on an electrode in contact with an argon plasma with $n_0 = 2.6 \times 10^{16}\,\mathrm{m}^{-3}$ and $T_e = 3\,\mathrm{eV}$.[14] Tailored rf bias voltage waveforms (at a frequency of 500 kHz, which corresponds to $\tau_i/\tau_{rf} < 1$) were applied to the electrode. The sheath was estimated to be thinner than the Ar^+ ion mean free path, minimizing ion collisions in the sheath. Fig. 3 shows a comparison of the voltage waveforms applied to the target electrode used in the experiments in Ref. 11 (left), with the model waveforms (right) used as input in the present calculations.

The voltage waveform used in the model was either a sine-wave raised to the power of m, to represent a spike, or two Fermi-Dirac distributions to represent a voltage step-up

Downloaded 03 Jul 2012 to 129.7.205.168. Redistribution subject to AIP license or copyright; see http://jap.aip.org/about/rights_and_permissions

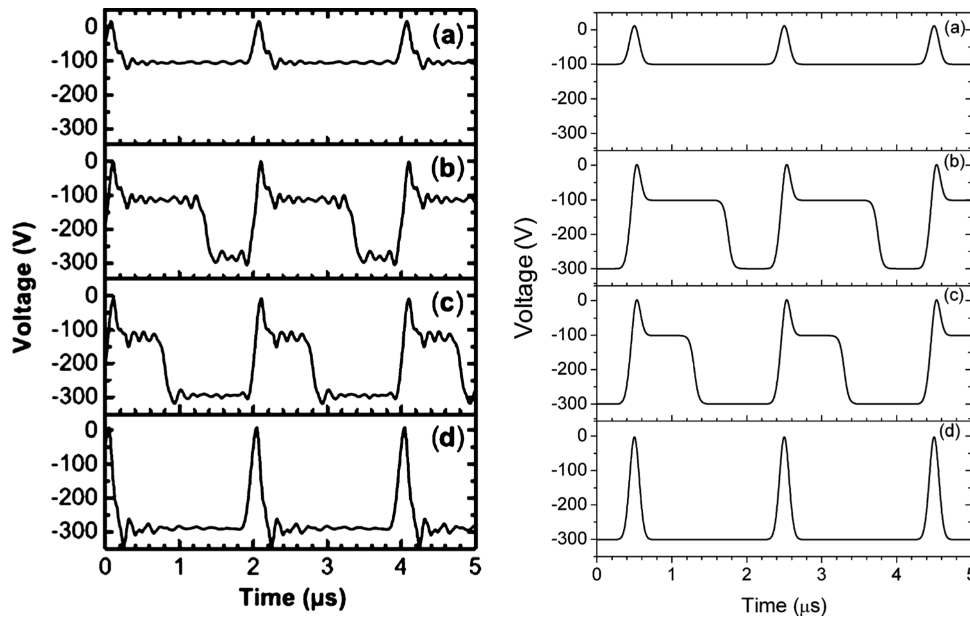

FIG. 3. (left) Experimental target voltage waveforms of Ref. 11. Reprinted with permission from X. V. Qin *et al.*, Plasma Sources Sci. Technol., **19**, 065014 (2010). Copyright © 2010 Institute of Physics Publishing; (right) model fit of the experimental waveforms used in the present calculations.

and step-down.[13] The analytical expression for the applied voltage for one cycle was

$$V_{rf}(t) = +V_a + V_b\left(\frac{1}{e^{[(-t+t_1)/\Delta t]}+1} + \frac{1}{e^{[(t-t_2)/\Delta t]}+1} - 1\right) + V_c \sin^m(\pi f_0(t+t_1)). \tag{12}$$

For the particular case of Fig. 3, the common parameter values were $f_0 = 500\,\text{kHz}$, $t_1 = 0.5\,\mu\text{s}$, m = 100, $\Delta t = 3\times10^{-8}\,\text{s}$. For the case in Fig. 3(a), $V_a = -100\,\text{V}$, $V_b = 0$, $V_c = 100\,\text{V}$; for the case in Figs. 3(b) and 3(c), $V_a = -300\,\text{V}$, $V_b = 200\,\text{V}$, $V_c = 175\,\text{V}$; and for the case in Fig. 3(d), $V_a = -300\,\text{V}$, $V_b = 0$, $V_c = 300\,\text{V}$. The value of t_2 was 1.75 μs and 1.3 μs for the case of Figs. 3(b) and 3(c), respectively. The simulated voltage waveforms (Fig. 3, right) are quite representative of the measured waveforms except for the "ringing." Since direct coupling was made to the electrode in the experiments (no blocking capacitor), $V_{rf} = V_T$ (see Fig. 2). Also, in this case $\tau_i/\tau_{rf} < 1$, and ions respond to the actual sheath potential, resulting in $V_d \approx V_T - V_p$. With V_{rf} given by Eq. (12), the calculated IEDs are compared to measurements in Fig. 4. The experimental energy resolution (bin size) of 1 eV was used in the model. Following the original Ref. 11, ΔE in Eq. (10) was set equal to 10 eV to account for plasma potential fluctuations.

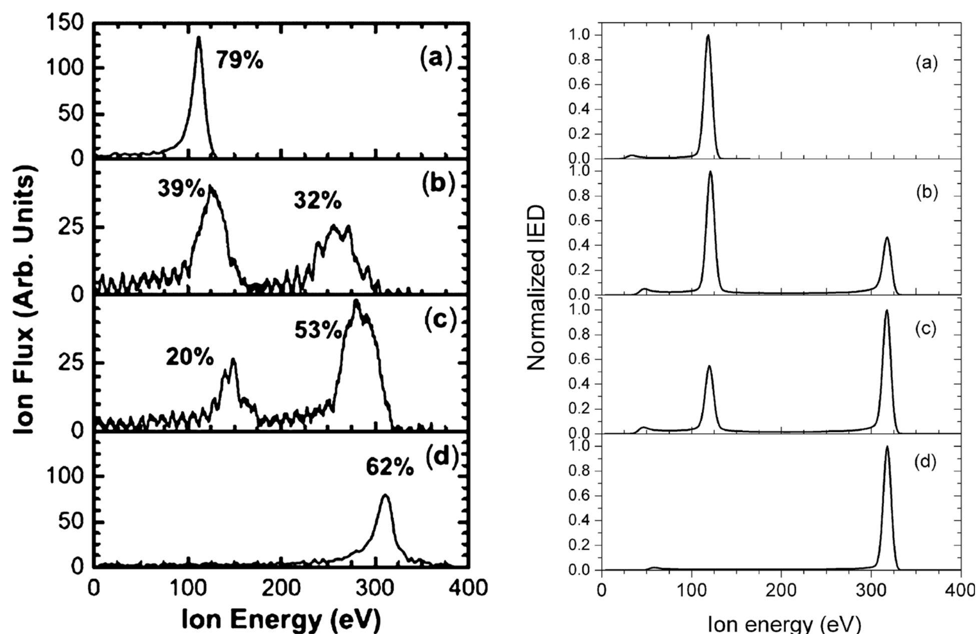

FIG. 4. Measured IEDs corresponding to the tailored bias waveforms shown in Fig. 3 (left).[11] Reprinted with permission from X. V. Qin *et al.*, Plasma Sources Sci. Technol., **19**, 065014 (2010). Copyright © 2010 Institute of Physics Publishing; calculated IEDs for the tailored bias waveforms shown in Fig. 3 (right).

Downloaded 03 Jul 2012 to 129.7.205.168. Redistribution subject to AIP license or copyright; see http://jap.aip.org/about/rights_and_permissions

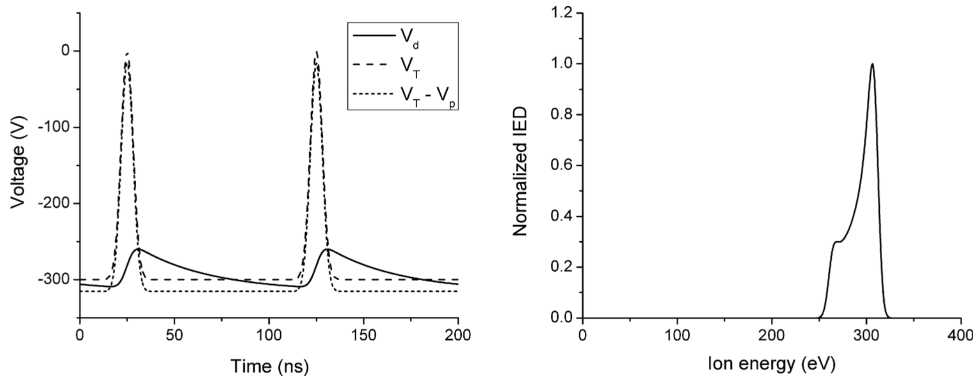

FIG. 5. (left) Damped (V_d), sheath ($V_T - V_p$), and applied (V_{rf}) potentials for the conditions of Fig. 3(d), except that $f_0 = 10$ MHz and $t_1 = 25$ ns; (right) resulting IED on target electrode.

The predicted peak locations and heights of the IED (Fig. 4, right) are in reasonable agreement with the measurements (Fig. 4, left). The FWHM of the experimental peaks are larger, most likely because of the fluctuations (ringing) of the applied voltage waveforms (Fig. 3, left). These fluctuations are not present in the waveforms used for simulations (Fig. 3, right). The staircase-like voltage waveform generates two peaks in the IED at energies controlled by the potential of the stairs. The brief peak near zero potential is designed to achieve a zero net current through the electrode. The fraction of ions at a particular energy can be controlled by changing the fraction of time the waveform spends at the corresponding value of potential.

The voltage waveform of Fig. 3(d) was also used to calculate the IED for an applied frequency of 10 MHz, corresponding to $t_1 = 25$ ns. ΔE in Eq. (10) was set equal to 10 eV. In this case, as shown in Fig. 5 (left), the damped potential and the sheath potential have different waveforms (ions do not follow the instantaneous sheath potential). The IED (Fig. 5, right) resembles a bimodal distribution with relatively small energy spread. The low energy peak is smeared by the relatively large broadening implied by $\Delta E = 10$ eV.

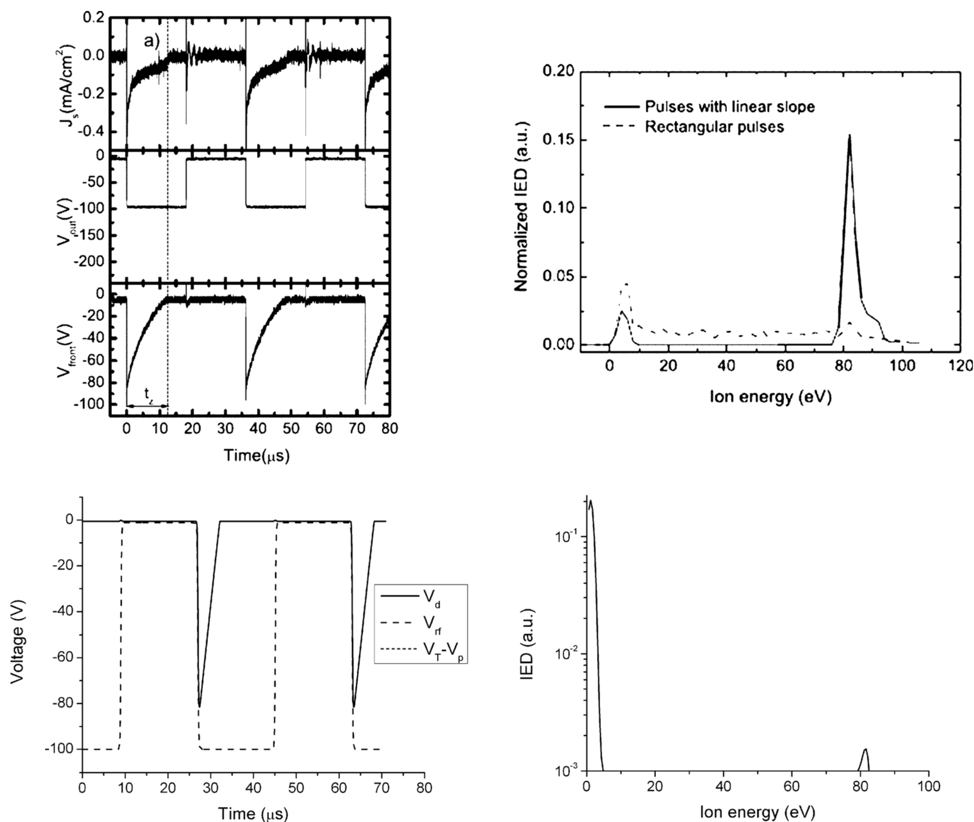

FIG. 6. (top left) Measured waveforms of substrate current density J_s (top), applied voltage V_{out} (middle), and the resulting substrate sheath voltage V_{front} (bottom), on a dielectric substrate.[15] Reprinted with permission from P. Kudlacek *et al*., J. Appl. Phys., **106**, 073303 (2009). Copyright © 2009 American Institute of Physics; (bottom left) calculated damped (V_d) and sheath ($V_T - V_p$) potentials, when the (V_{rf}) waveform (corresponding to V_{out}) is applied on the target electrode; (top, right) estimated[15] energy distributions of ions bombarding the substrate (only the dashed line is relevant for this case). Reprinted with permission from P. Kudlacek *et al*., J. Appl. Phys., **106**, 073303 (2009). Copyright © 2009 American Institute of Physics; (bottom, right) IED predicted by the present model.

Downloaded 03 Jul 2012 to 129.7.205.168. Redistribution subject to AIP license or copyright; see http://jap.aip.org/about/rights_and_permissions

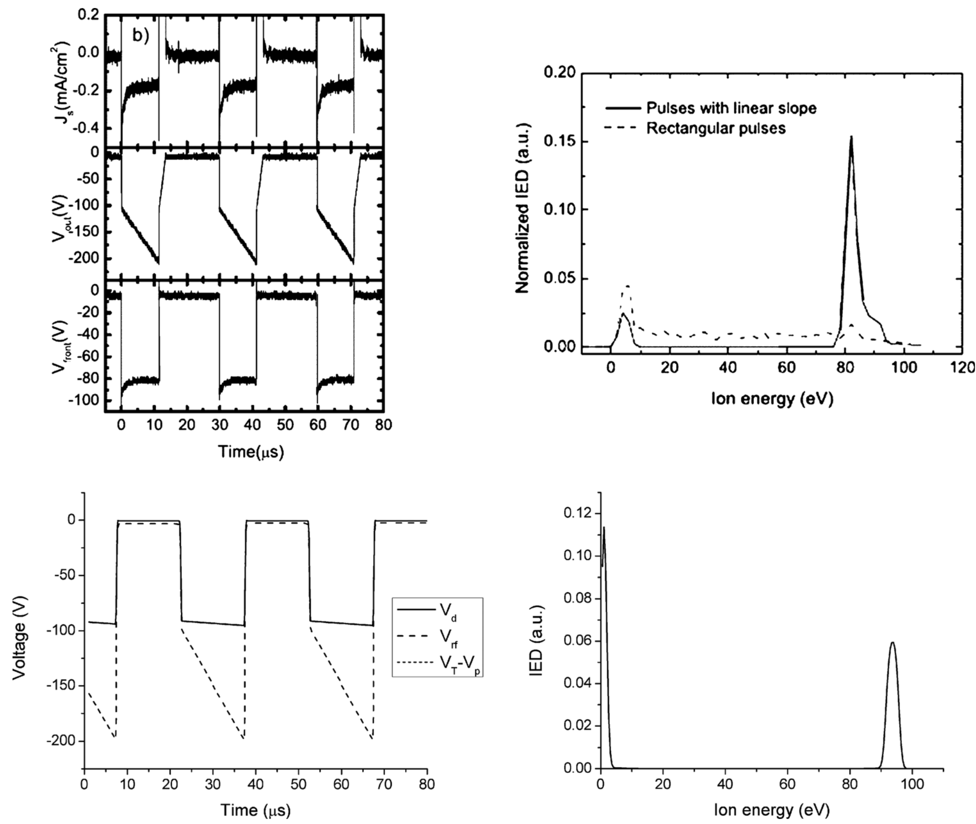

FIG. 7. (top, left) Measured waveforms of substrate current density J_s (top), applied voltage V_{out} (middle), and the resulting substrate sheath voltage V_{front} (bottom), on a dielectric substrate.[15] Reprinted with permission from P. Kudlacek *et al*., J. Appl. Phys., **106**, 073303 (2009). Copyright © 2009 American Institute of Physics; (bottom, left) calculated damped (V_d) and sheath ($V_T - V_p$) potentials, when the V_{rf} waveform (corresponding to V_{out}) is applied on the target electrode; (top, right) estimated[15] energy distributions of ions bombarding the substrate (only the solid line is relevant for this case). Reprinted with permission from P. Kudlacek *et al*., J. Appl. Phys., **106**, 073303 (2009). Copyright © 2009 American Institute of Physics; (bottom, right) IED predicted by the present model.

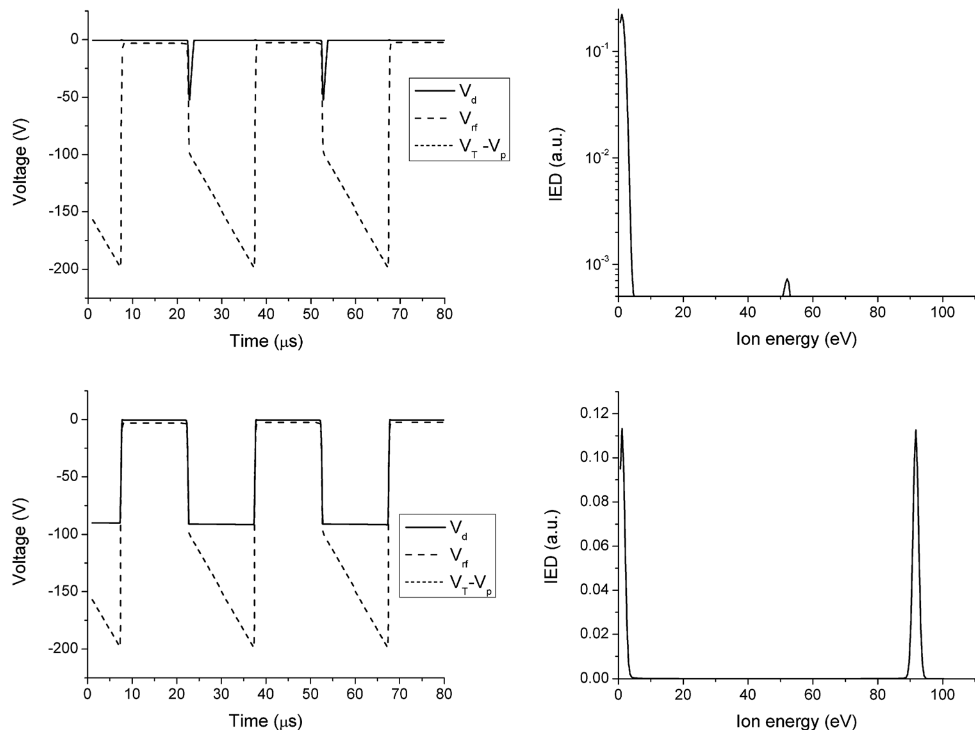

FIG. 8. Damped (V_d), sheath ($V_T - V_p$), and applied (V_{rf}) potentials on the target electrode (left), and predicted IED (right), for a square wave with a constant slope applied to a dielectric substrate. (top) $C_b = 166\,\text{pF}$; (bottom) $C_b = 1.6\,\text{nF}$.

Downloaded 03 Jul 2012 to 129.7.205.168. Redistribution subject to AIP license or copyright; see http://jap.aip.org/about/rights_and_permissions

B. Square wave

Further comparisons were made with the experimental results of Kudlacek *et al.*[15] They were interested in the IEDs on a substrate downstream of an expanding hydrogen thermal plasma at a position of very low plasma potential (0.2 V) and electron temperature (0.15 eV). The plasma density over the substrate was $\sim 2 \times 10^{10}$ cm^{-3} at a pressure of 18 Pa. The authors applied rectangular voltage waveforms with a frequency of 27.7 kHz and 50% duty cycle applied to a dielectric substrate with a capacitance of 166 pF. In one particular case, the voltage during the pulse ON phase was −100 V and that during the OFF phase V_{off} was the floating potential, V_f, equal to −2 V. This voltage was represented with Eq. (12) using $t_1 = 9\,\mu$s, $t_2 = 27\,\mu$s, $\Delta t = 8.5 \times 10^{-8}$ s, $V_a = -100$ V, $V_b = 98$ V, and $V_c = 0$. The area ratio was 25. The measured IEDs (the predominant ion was H_3^+) are compared to those calculated with the present model in Fig. 6. The energy resolution of the measurement and the FWHM of the instrumental broadening were estimated to be 0.5 eV and 2 eV,[15] respectively. These values were used for all cases in this subsection. Since the condition $\tau_i/\tau_{rf} < 1$ is again satisfied, the damped sheath potential V_d is almost identical to the actual sheath potential, $V_T - V_p$. The model is capable of matching the energies corresponding to the maximum of the two peaks, and also the triangular waveform of the target voltage (Fig. 6), by using a capacitance $C_b = 600$ pF, higher than that of the dielectric substrate. The difference may be explained by stray capacitance which should be in parallel with that of the substrate, making the total actual capacitance larger.

Further comparison with the experiments in Ref. 15 was made for the case of a dielectric-covered substrate for an applied voltage waveform (at 33.3 kHz with 50% duty cycle) consisting of a rectangular pulse with a slope (Fig. 7). The parameter values $t_1 = 7.5\,\mu$s, $t_2 = 22.5\,\mu$s, and $\Delta t = 8.5 \times 10^{-8}$ were used in Eq. (12) to reproduce the applied voltage waveform. The area ratio was set at 25, and $C_b = 1.66$ nF. The model is again able to predict the position of the peaks of the IED and the almost square waveform target voltage measured experimentally (Fig. 7), albeit with a blocking capacitance higher (1.66 nF vs. 166 pF) than that of the substrate alone.[15]

The effect of variation of the blocking capacitance can be observed in Fig. 8. For $C_b = 166$ pF, both the actual and the damped sheath voltage have a triangular shape, and the IED has a very small peak (note log scale in Fig. 8, bottom right) near 50 eV and a large peak at very low energies, in contrast with the results of Ref. 15. For $C_b = 1.6$ nF, an almost perfect square wave is obtained for the damped potential.

C. Pulsed discharge with synchronous dc bias in the afterglow

This section compares modeling results with the experimental data of Shin *et al.*[5] They measured IEDs on a grounded substrate in a pulsed argon inductively coupled plasma (ICP). A 24.4 V dc bias was synchronously applied to a "boundary electrode" in contact with the plasma during part of the afterglow of the pulsed discharge. The pulse period was 100 μs, the duty cycle was 20% and the dc bias was

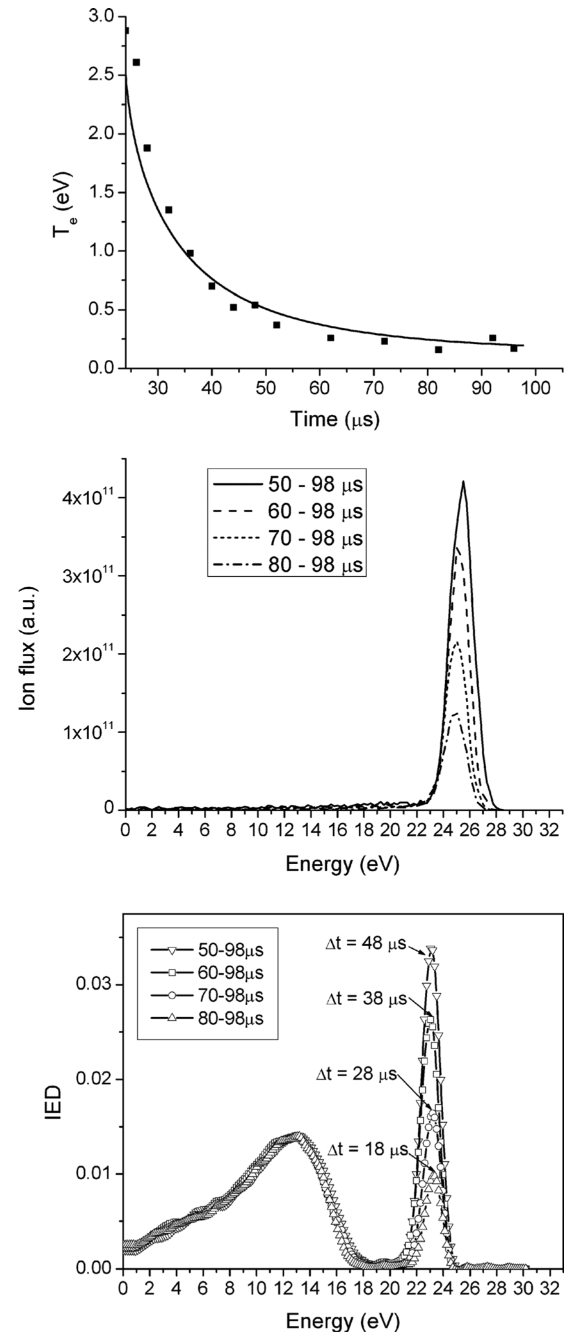

FIG. 9. (top) Comparison between the PIC/MCC simulation (solid line) and experimental data (closed squares) of electron temperature decay in the afterglow; calculated (middle) and measured (bottom) IED when a dc bias is applied in the afterglow with different starting time, but the same ending time. Only the afterglow was simulated by PIC-MCC; hence, the broad low energy peak corresponding to the active glow was not captured.

applied in the afterglow from $t = 45\,\mu$s to $t = 95\,\mu$s, where $t = 0$ corresponds to the start of plasma ON phase (thus, $t = 20\,\mu$s marks the start of the afterglow). The positive dc bias on the boundary electrode raises the plasma potential by a commensurate amount, thereby increasing the voltage of the sheath over the grounded substrate. During the afterglow, and in the absence of any bias, the plasma potential quickly diminishes to very low values. At that stage, application of a positive dc bias on the boundary electrode results in a plasma potential equal to the dc bias. This set up is equivalent to biasing the substrate (target) electrode with −24.4 V. A PIC-

Downloaded 03 Jul 2012 to 129.7.205.168. Redistribution subject to AIP license or copyright; see http://jap.aip.org/about/rights_and_permissions

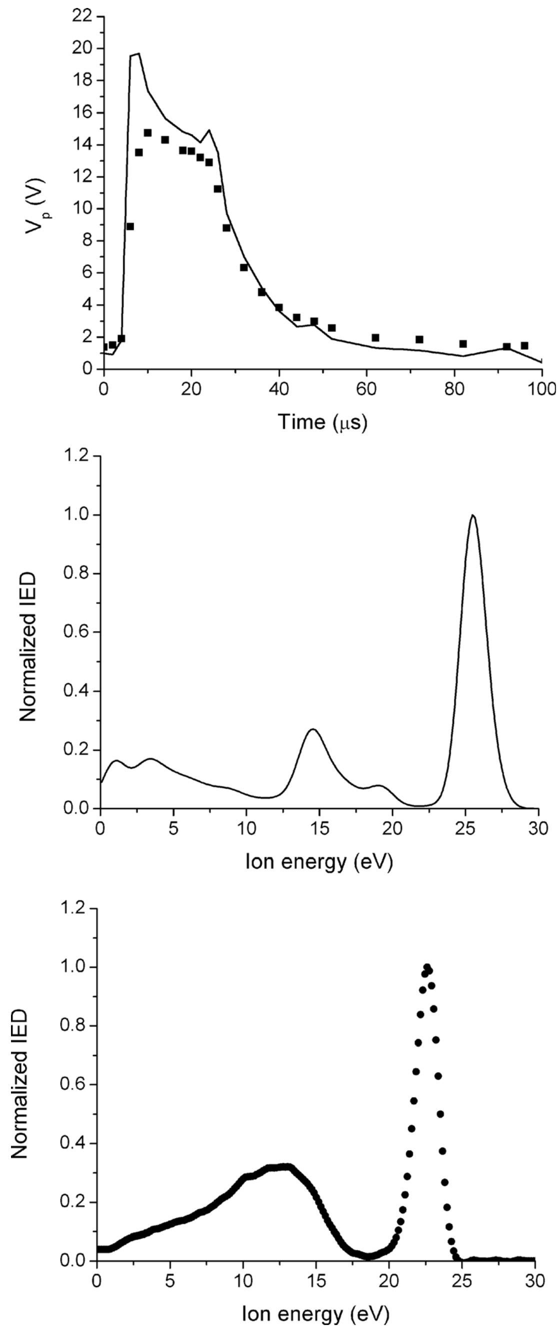

FIG. 10. (top) Comparison between the calculated (solid line) and measured (closed squares) plasma potential[5]; calculated (solid line, middle) and measured (closed circles, bottom) IED for 14 mTorr pressure.[5]

MCC was performed first.[21,29] Since ICP discharges are cumbersome to simulate to steady state with PIC-MCC (high plasma density and therefore very thin sheaths require extraordinarily long simulations times), a capacitively coupled plasma (CCP) was simulated instead as a surrogate system. Regardless of how a discharge is ignited, the plasma potential and the electron temperature will quickly decay in the afterglow. Thus, after some microseconds, the afterglow of an ICP discharge will be quite similar to that of a CCP discharge assuming their geometries and parameters such as gas pressure and plasma density at turn-off are comparable. A PIC-MCC simulation of a 14 mTorr, 60 MHz argon discharge in a parallel plate geometry (plate separation 6 cm) with 600 V applied peak RF voltage, gave a steady-state plasma density at the sheath edge equal to 3×10^{16} m^{-3}, comparable with the experimental value of 5×10^{16} m^{-3}. Fig. 9 shows a comparison of PIC-MCC simulation predictions with the data. The decay of electron temperature is captured, as well as the shape, location, and relative magnitude of the IED peaks in the afterglow. The simulation also predicts the magnitude of the FWHM of the IEDs. The width of the IED is affected by the physics of the problem (energy and angular distributions of ions entering the sheath, ion-neutral collisions in the sheath, etc.) as well as the instrument resolution. The FWHM predicted by the simulation is entirely due to the physics of the problem. It should be noted that the experimental IEDs have an additional peak at lower energy due to ions bombarding the substrate during the active glow and the fraction of the afterglow when there is no applied bias. The simulation could not capture the low energy peak since the active glow of the experimental ICP reactor was not simulated by PIC-MCC, and ion collection was done only during the dc bias application window in the afterglow.

The model developed in this work was also used to predict the experimental IED in the afterglow. The electron density n_e and electron temperature T_e were measured as a function of time, and used as input to the model. The following parameters were used in Eq. (12) to emulate the applied bias: $t_1 = 95\,\mu$s, $t_2 = 45\,\mu$s, $\Delta t = 3 \times 10^{-7}$ s, $V_a = 0$, $V_c = 0$, and $V_b = 24.4$ V for one cycle from $t = 0$ to $t = 100\,\mu$s at the pulsing frequency of 10 kHz. The bias was dc coupled to the electrode (no blocking capacitor). The energy grid resolution was 0.15 eV and the FWHM of the IED was taken as 1.9 eV, equal to that predicted by the PIC-MCC simulation. (It was found that the IED can be represented by a Gaussian (Eq. (9)) even when the FWHM is dominated by other than instrumental broadening.) The model reproduces the experimentally measured rise and decay of the plasma potential as a function of time (Fig. 10). The spike in the plasma potential at plasma turn-on predicted by the model mirrors a corresponding spike in the measured electron temperature. The calculated IEDs are in good agreement with the experiments, except that the model predicts a few minor peaks (e.g., below 5 eV) that are not seen experimentally. The small peaks in the IED near 1 and 3 eV are due to the period when no dc bias was applied to the electrode. Similar agreement was obtained at other pressures as well. The lack of very low energy (<5 eV) peaks in the measured IED may be an experimental artifact.

The retarding field energy analyzer employed in the experiments incorporated a negatively biased grid above the ion energy selector grid.[5] Very low energy ions can be easily deflected and collected by the negatively biased grid. In addition, very low energy ions have larger angles of divergence and may be preferentially filtered out at the entrance to the analyzer facing the plasma. Very low energy peaks in the IED were also observed using a hybrid simulation of this experimental apparatus.[30]

IV. SUMMARY

A model was developed, allowing rapid calculation of the IED on an electrode immersed in plasma, for given

Downloaded 03 Jul 2012 to 129.7.205.168. Redistribution subject to AIP license or copyright; see http://jap.aip.org/about/rights_and_permissions

voltage waveform applied to the electrode through a blocking capacitor. The model combined an equivalent circuit representation of the system, with an equation for a "damped" sheath potential to which ions respond. The damped sheath potential was identical to the actual sheath potential when $\tau_{rf}/\tau_i \gg 1$, where τ_{rf} and τ_i are the period of the RF voltage applied to the electrode and the ion transit time through the sheath, respectively. The resolution of the ion energy analyzer was also taken into account, but ion-neutral collisions in the sheath were neglected. Therefore, the model is applicable for $\lambda_i/L \gg 1$, where λ_i is the ion mean free path and L is the sheath thickness. The model results agree well with results obtained by more computationally expensive methods (PIC-MCC and hybrid simulations) that can in any case be used to estimate the broadening of the IED due to physical effects that cannot be included in the circuit model. Predicted IEDs on both conducting and insulating electrodes for a variety of applied voltage waveforms (spike, staircase, square wave, etc.) were in agreement with published experimental data. Using judiciously selected voltage waveforms, one may achieve a desired IED. For example, an IED with two isolated energy peaks and with controlled fraction of ions under each peak may be obtained by using a staircase voltage waveform, with controlled levels of potentials (equal to the desired peak ion energy) and variable fraction of time spent in each potential. In all cases, the waveform should spike towards ground for a short time to allow sufficient electron current to neutralize the positive ion current flowing to the electrode. On insulating electrodes, the potential has to become more negative as a function of time to counterbalance the inevitable charging of the electrode surface.

ACKNOWLEDGMENTS

This work was supported by the Department of Energy, Office of Fusion Energy Science, Contract DE-SC0001939, the National Science Foundation Grant CBET 0903426, the Department of Energy Grant DE-SC0000881, and the NSF Grant CMMI 1030620.

[1]E. Kawamura, V. Vahedi, M. A. Lieberman, and C. K. Birdsall, Plasma Sources Sci. Technol. **8**, R45 (1999).
[2]T. Panagopoulos and D. J. Economou, J. Appl. Phys. **85**, 3435 (1999).
[3]E. A. Edelberg and E. S. Aydil, J. Appl. Phys. **86**, 4799 (1999).
[4]L. Xu, D. J. Economou, V. M. Donnelly, and P. Ruchhoeft, Appl. Phys. Lett. **87**, 041502 (2005).
[5]H. Shin, W. Zhu, L. Xu, D. J. Economou, and V. M. Donnelly, Plasma Sources Sci. Technol. **20**, 055001 (2011).
[6]K.-U. Riemann, Phys. Fluids **24**, 2163 (1981).
[7]S. K. Nam, D. J. Economou, and V. M. Donnelly, Plasma Sources Sci. Technol. **16**, 90 (2007).
[8]E. V. Barnat and T.-M. Lu, J. Vac. Sci. Technol. A **17**, 3322 (1999).
[9]E. V. Barnat and T.-M. Lu, Phys. Rev. E **66**, 056401 (2002).
[10]E. V. Barnat and T.-M. Lu, J. Appl. Phys. **92**, 2984 (2002).
[11]X. V. Qin, Y.-H. Ting, and A. E. Wendt, Plasma Sources Sci. Technol. **19**, 065014 (2010).
[12]M. M. Patterson, H.-Y. Chu, and A. E. Wendt, Plasma Sources Sci. Technol. **16**, 257 (2007).
[13]S.-B. Wang and A. E. Wendt, J. Appl. Phys. **88**, 643 (2000).
[14]F. L. Buzzi, Y.-H. Ting, and A. E. Wendt, Plasma Sources Sci. Technol. **18**, 025009 (2009).
[15]P. Kudlacek, R. F. Rumphorst, and M. C. M. van de Sanden, J. Appl. Phys. **106**, 073303 (2009).
[16]I. T. Martin, M. A. Wank, M. A. Blauw, R. A. C. M. M. van Swaaij, W. M. M. Kessels, and M. C. M. van de Sanden, Plasma Sources Sci. Technol. **19**, 015012 (2010).
[17]M. A. Wank, R. A. C. M. M. van Swaaij, P. Kudlacek, M. C. M. van de Sanden, and M. Zeman, J. Appl. Phys. **108**, 103304 (2010).
[18]A. Agarwal and M. J. Kushner, J. Vac. Sci. Technol. A **23**, 1440 (2005).
[19]S. Rauf, J. Appl. Phys. **87**, 7647 (2000).
[20]E. V. Johnson, T. Verbeke, J.-C. Vanel, and J.-P. Booth, J. Phys. D: Appl. Phys. **43**, 412001 (2010).
[21]P. Diomede, D. J. Economou, and V. M. Donnelly, J. Appl. Phys. **109**, 083302 (2011).
[22]P. Diomede, M. Nikolaou, and D. J. Economou, Plasma Sources Sci. Technol. **20**, 045011 (2011).
[23]A. Metze, D. W. Ernie, and H. J. Oskam, J. Appl. Phys. **60**, 3081 (1986).
[24]A. Metze, D. W. Ernie, and H. J.Oskam, J. Appl. Phys. **65**, 993 (1989).
[25]P. Miller and M. Riley, J. Appl. Phys. **82**, 3689 (1997).
[26]B. Chapman, *Glow Discharge Processes* (J. Wiley, New York, 1980).
[27]M. Sobolewski, Phys. Rev. E **62**, 8540 (2000).
[28]T. Baloniak, R. Reuter, and A. von Keudell, J. Phys. D: Appl. Phys. **43**, 335201 (2010).
[29]J. Verboncoeur, M. V. Alves, V. Vahedi, and C. K. Birdsall, J. Comp. Phys. **104**, 321 (1993).
[30]M. D. Logue, H. Shin, W. Zhu, L. Xu, V. M. Donnelly, D. J. Economou, and M. J. Kushner, "Ion energy distributions in pulsed inductively-coupled plasmas having a pulsed boundary electrode," in *Bulletin of the APS, 64th Annual Gaseous Electronics Conference*, Salt Lake City, UT, 14–18 November 2011, http://meetings.aps.org/link/BAPS.2011.GEC.LW3.6.

Downloaded 03 Jul 2012 to 129.7.205.168. Redistribution subject to AIP license or copyright; see http://jap.aip.org/about/rights_and_permissions